Molecular orientation transition of organic thin films on graphite: the effect of intermolecular electrostatic and interfacial dispersion forces

Wei Chen,* Han Huang, Andrew Thye and Shen Wee*

Received (in Cambridge, UK) 7th April 2008, Accepted 5th June 2008
First published as an Advance Article on the web 16th July 2008
DOI: 10.1039/b805788e

***In situ* low-temperature scanning tunnelling microscopy investigation reveals a molecular orientation transition of organic thin films of pentacene and *p*-sexiphenyl on graphite, arising from the delicate balance between the intermolecular electrostatic and interfacial dispersion forces.**

Thin films based organic electronic devices have been successfully demonstrated in low-cost, large-scale and flexible electronics.[1] The electronic properties of organic thin films, in particular the charge transport, largely depend on the supramolecular arrangement and thin film morphology in the solid state.[1–7] However, the supramolecular arrangement or molecular orientation in these van der Waals bonded organic thin films is generally difficult to control and is a major challenge in this field. Two important factors determine the molecular orientation in organic thin films: (i) molecule–substrate interfacial interactions; and (ii) intermolecular interactions. Intensive research has been devoted to understand the effect of the molecule-substrate interfacial interactions on the molecular orientation of organic thin films.[8–14] It was found that the coupling between molecular orbitals and substrate valence or conduction bands plays a crucial role in determining the molecular orientation.

The intermolecular interactions for widely used π-conjugated molecules such as pentacene, tetracene, oligo-thiophenes, oligo-phenyls and phthalocyanines are usually dominated by intermolecular π–π interactions, which can be decomposed into long-range dispersion and electrostatic forces and short-range charge transfer interactions.[15] It is generally accepted that the intermolecular electrostatic force or the quadrupole–quadrupole interaction gives rise to the herringbone arrangement of most organic single crystals.[15–17] The intermolecular dispersion force also plays an important role in determining the molecular orientation in organic thin films, in particular for the disk-like planar π-conjugated molecules such as various phthalocyanines.[18] The collective effect of the dispersion and electrostatic forces leads to the formation of weakly bonded van der Waals organic crystals or thin films with well-defined molecular orientations.[18]

Interfacial interactions between the chemically inert graphite surface and π-conjugated molecules are dominated by π–π interactions, *i.e.*, dispersion and electrostatic forces. Hence, molecular adsorption on graphite is an ideal model system to study how intermolecular π–π interactions affect molecular self-assembly and molecular orientation on surfaces. The interplay between intermolecular and interfacial interactions results in a rich variety of growth behaviors of organic thin films. Careful inspection of various supramolecular packing structures on graphite surface can provide detailed information on how intermolecular interactions determine molecular orientation in organic thin film growth. In this paper, *in situ* low-temperature scanning tunneling microscopy (LT-STM) is used to monitor the thickness-dependent molecular packing and orientation of rod-like pentacene ($C_{22}H_{14}$) and 6P ($C_{36}H_{26}$) layers on highly ordered pyrolytic graphite (HOPG) substrates.

The LT-STM experiments were carried out in a custom-built multi-chamber ultra-high-vacuum (UHV) system housing an Omicron LT-STM interfaced to a Nanonis controller (Nanonis, Switzerland).[19] All STM imaging were performed at 77 K. 6P and pentacene were deposited from two Knudsen cells at room temperature (RT) in a separate growth chamber. The deposition rates of 6P and pentacene were monitored by a quartz-crystal-microbalance (QCM) during evaporation. In our experiments, all depositions were performed at constant rates of about 0.01 ML min^{-1} for 6P and 0.015 ML min^{-1} for pentacene (1 monolayer = one full monolayer of close packed 6P or pentacene with their conjugated π-plane oriented parallel to HOPG surface).

In situ LT-STM was used to monitor the supramolecular packing of organic thin films on HOPG as a function of coverage. Fig. 1(a) shows a representative molecularly-resolved 30 × 30 nm^2 STM image of a well-ordered pentacene monolayer on HOPG, in which each rod-like bright feature represents a single pentacene molecule. Perfectly ordered pentacene monolayer with a lying-down configuration forms on HOPG. Fig. 1(b) displays

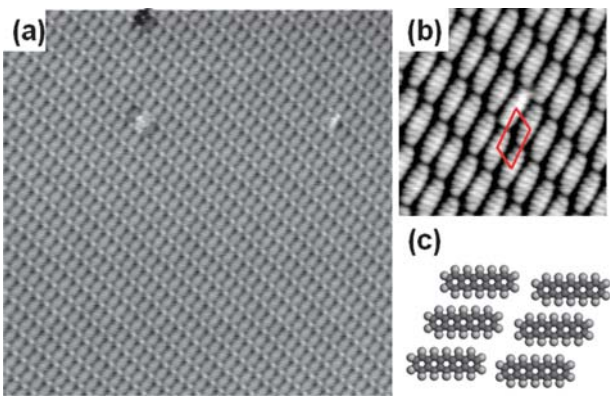

Fig. 1 STM images for lying-down pentacene monolayer on HOPG surface (30 × 30 nm^2, V_{tip} = −2.0 V) and (b) shows the corresponding detailed 8 × 8 nm^2 image (V_{tip} = −1.6 V). (c) Schematic drawing for the proposed molecular packing structure of lying-down pentacene on HOPG.

Department of Physics, National University of Singapore, 2 Science Drive 3, 117542, Singapore. E-mail: phycw@nus.edu.sg; phyweets@nus.edu.sg; Fax: +65-67776126; Tel: +65-65161879

 This journal is © The Royal Society of Chemistry 2008

the corresponding molecular-resolved 8 × 8 nm^2 STM image, clearly showing that all pentacene molecules lie flat on the substrate with their extend π-plane parallel to the surface.[20,21] The unit cell is highlighted in Fig. 1(b) with $a = 0.89 \pm 0.05$ nm, $b = 1.63 \pm 0.05$ nm, and $\alpha = 60 \pm 2°$. The schematic drawing in Fig. 1(c) shows the proposed molecular packing structure for the pentacene monolayer on HOPG.

When the pentacene coverage increases beyond one monolayer, instead of retaining the lying-down configuration, a new long-range ordered supramolecular structure with a smaller unit cell forms, as shown by the 20 × 20 nm^2 STM image in Fig. 2(a) and the corresponding detailed 5 × 5 nm^2 STM image in Fig. 2(b). The unit cell is highlighted in Fig. 2(b) with $a = 0.57 \pm 0.05$ nm, $b = 0.79 \pm 0.05$ nm, and $\alpha = 88 \pm 2°$. This images matches previously reported STM images of the standing-up pentacene thin film on Bi(001) with their long molecular axis normal to the surface plane,[14] referred to as the head-on configuration. The head-on pentacene molecules adopt a herringbone arrangement as typically observed for pentacene thin films on passivated or weakly interacting substrates such as SiO_2.[11,16] Fig. 2(c) and (d) display the schematic drawings for the proposed molecular packing structure of the standing-up pentacene layer on HOPG in top view and side view, respectively.

It is known that the non-local dispersion force plays an important role in stabilizing the adsorption of organic molecules on weakly interacting substrates and gives rise to the lying-down configuration of disk-like planar π-conjugated molecules such as various phthalocyanines at the monolayer or submonolayer coverages.[15,18,22,23] As such, the well-ordered pentacene monolayer on HOPG with their extend π-plane parallel to the surface (Fig. 1) can be attributed to the interfacial dispersion force between pentacene and HOPG. It was reported that the intermolecular interactions result in the formation of two stable benzene-dimers, *i.e.*, T-shaped, and flipped-parallel dimers.[15] Although the intermolecular dispersion force contributes significantly to lowering the total energy of both dimers, the attractive intermolecular electrostatic force or the quadruple–quadruple interaction stabilizes the T-shaped benzene dimer.[15] It also gives rise to a herringbone arrangement of molecules in organic single crystals such as pentacene and oligo-thiophenes instead of π–π stacking.[15,18] Similarly, the formation of the head-on pentacene (standing-up) film with a typical herringbone arrangement on HOPG in Fig. 2 is driven by the intermolecular electrostatic force. The observed orientation transition of pentacene films on HOPG from the lying-down to the standing-up configurations arises from the delicate balance between the intermolecular electrostatic and interfacial dispersion forces at different coverages.

Similar thickness-dependent orientation transition has also been observed for 6P thin films on HOPG. Fig. 3(a) shows a representative molecularly-resolved 15 × 15 nm^2 STM image of a well-ordered 6P monolayer on HOPG, in which each rod-shape feature represents a single 6P molecule. The width of the 6P monolayer nanostripes is 2.95 ± 0.02 nm as highlighted in Fig. 3(a), which is close to the van der Waals length of 6P molecules (2.73 nm).[17] The periodicity along the 6P monolayer stacking direction (highlighted by the dashed line) is 0.70 ± 0.02 nm, as revealed by the line profile in Fig. 3(e). We propose a model involving side-by-side packing of 6P molecules with their extended π-plane parallel to the HOPG surface, as shown by the schematic drawing in Fig. 3(f). Such molecular packing is similar to that of α-sexithiophene (6T) on Ag(111) or HOPG and 6P on Ag(111),[19] and is referred to as the "face-on" 6P monolayer phase. The 6P-HOPG interface is dominated by dispersion force, which contributes to lower the total energy of

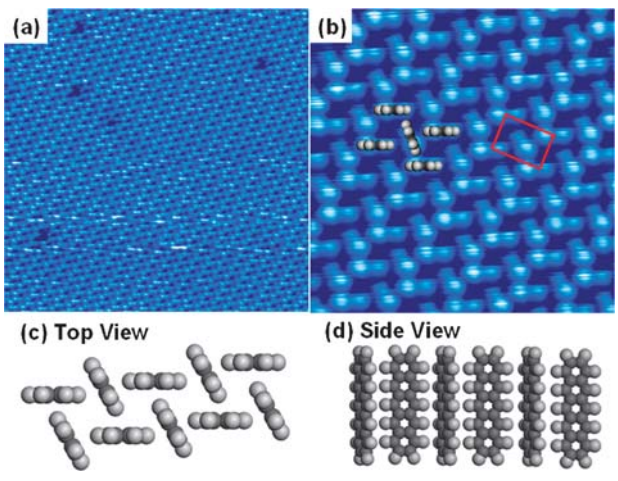

Fig. 2 STM images for standing-up pentacene layer on HOPG surface: (a) 20 × 20 nm^2, and (b) 5 × 5 nm^2 image, $V_{tip} = 0.8$ V for both images. The square highlights the unit cell. (c) and (d) schematic drawings for the proposed molecular packing structure of standing-up pentacene layer on HOPG in top view and side view, respectively.

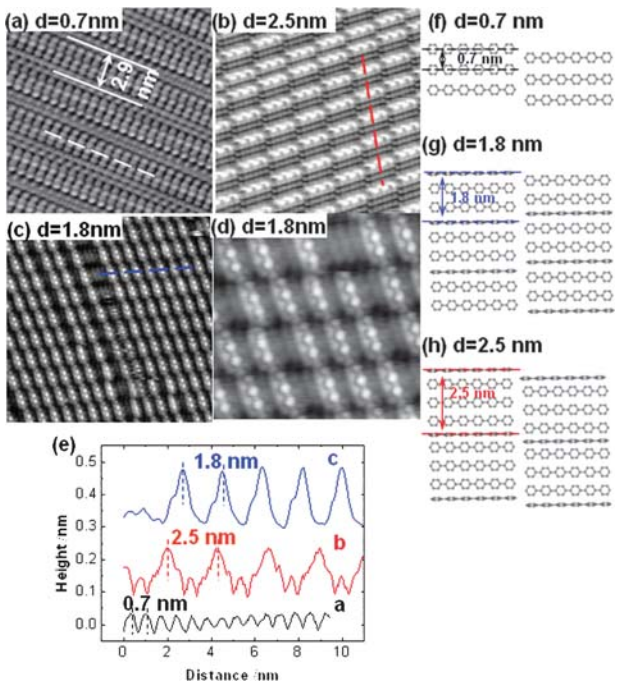

Fig. 3 Thickness-dependent STM images of 6P on HOPG surface. (a) "face on" 6P monolayer, 15 × 15 nm^2, $V_{tip} = -1.5$ V; (b) "face-on + edge-on" 6P layer with 2.5 nm inter-stripe distance, 20 × 20 nm^2, $V_{tip} = +3.3$ V; (c) "face-on + edge-on" 6P layer with 1.8 nm inter-stripe distance, 30 × 30 nm^2, $V_{tip} = -3.2$ V, and (d) corresponding detailed 12 × 12 nm^2 image for panel (c). (e) Corresponding line profiles as indicated by the dashed line in panels (a), (b) and (c). Panels (f), (g) and (h): Corresponding schematic models for the supramolecular arrangement of 6P molecules on HOPG in panels (a), (b) and (c), respectively.

the adsorption system and stabilizes the "face-on" 6P monolayer on HOPG.

It has been reported that increasing the 6P coverage leads to the insertion of edge-on 6P into the face-on 6P monolayer on Au(111) forming a more compact molecular packing phase.[24] The edge-on configuration refers to 6P molecules orientated with their phenyl rings perpendicular to the surface, and long molecular axis parallel to the surface. Such alternating arrangements of face-on and edge-on 6P molecules is reminiscent of the typical herringbone structure commonly observed in 6P single-crystal solids, stabilized by the electrostatic force between neighboring face-on and edge-on 6P molecules.[15,24] A similar growth behavior has also been observed for 6P on HOPG. Depositing 0.10 ML 6P on the "face-on" 6P monolayer on HOPG leads to the formation of 6P nanostripes with a larger intermolecular spacing of 2.5 ± 0.02 nm along the 6P packing direction (highlighted by the dashed line) in Fig. 3(b) and the corresponding line profile in Fig. 3(e). The proposed model is shown in Fig. 3(g), which involves an alternating arrangement of one edge-on 6P and three successive face-on 6P molecules. Increasing the 6P coverage to 0.15 ML on the "face-on" 6P monolayer results in a more compact 6P nanostripe array as shown in Fig. 3(c) and (d). The periodicity along the molecular packing direction is 1.8 ± 0.02 nm, as revealed by the line profile in Fig. 3(e). As shown in Fig. 3(d), the "edge-on" 6P molecules adopt a "zigzag" pattern along the molecular axis. This suggests that the neighboring phenyl rings in the "edge-on" 6P molecule are twisted with respect to each other.[25] Fig. 3(h) displays the corresponding schematic model for this 6P array, which comprises a periodic arrangement of a face-on 6P pair with a single edge-on 6P molecule. Moreover, it is possible to tune the periodicity along the molecular packing direction of the 6P nanostripe array by careful control of the coverage of inserted edge-on 6P molecules, showing the potential of this system as an effective dynamic molecular surface nanotemplate.

In conclusion, *in situ* LT-STM has been used to study the molecular orientation transition of organic thin films of pentacene and 6P on chemically inert HOPG surface. Dispersion force dominates the molecule–HOPG interfaces below one monolayer coverage, causing 6P and pentacene molecules to adopt the lying-down configuration with their extended π-planes oriented parallel to the surface. Beyond one monolayer coverage, the intermolecular electrostatic force leads to the insertion of the edge-on 6P molecules into the face-on 6P layer; while the more rigid pentacene molecules prefer the head-on configuration with their long molecular axis perpendicular to the surface plane and form a herringbone arrangement. This investigation helps us to understand and control the molecular orientation in organic thin films on various dielectric, metal electrodes surfaces, and at organic heterojunction interfaces. This knowledge will enable us to optimize the efficient charge transport or light absorption of these thin films, for potential applications in organic field-effect-transistors, organic light-emitting-diodes and organic solar cells.

Dr W. Chen acknowledges the financial support by LKY PDF fellowship. Authors acknowledge the support from the A*STAR grant R-398-000-036-305 and ARF grant R-144-000-196-112.

Notes and references

1 C. D. Dimitrakopoulos and P. R. L. Malenfant, *Adv. Mater.*, 2002, **14**, 99; S. R. Forrest, *Nature*, 2004, **428**, 911; S. R. Forrest, *MRS Bull.*, 2005, **30**, 28; M. A. Muccini, *Nat. Mater.*, 2006, **5**, 605; J. A. Rogers, *Science*, 2001, **291**, 1502.
2 F. Dinelli, R. Capelli, M. A. Loi, M. Murgia, M. Muccini, A. Facchetti and T. J. Marks, *Adv. Mater.*, 2006, **18**, 1416.
3 V. Coropceanu, J. Cornil, D. A. da Silva, Y. Olivier, R. Silbey and J. Bredas, *Chem. Rev.*, 2007, **107**, 926.
4 K. O. Sylvester-Hvid, *J. Phys. Chem. B*, 2006, **110**, 2618.
5 V. de Bettignies, Y. Nicolas, P. Blanchard, E. Levillain, J.-M. Nunzi and J. Roncali, *Adv. Mater.*, 2003, **15**, 1939.
6 C. Videlot, A. El Kassmi and D. Fichou, *Sol. Energy Mater. Sol. Cells*, 2000, **63**, 69.
7 S. Heutz, C. Mitra, W. Wu, A. J. Fisher, A. Kerridge, M. Stoneham, T. H. Harker, J. Gardener, H.-H. Tseng, T. S. Jones, C. Renner and G. Aeppli, *Adv. Mater.*, 2007, **19**, 3618.
8 A. Kraft, R. Temirov, S. K. M. Henze, S. Soubatch, M. Rohlfing and F. S. Tautz, *Phys. Rev. B*, 2006, **74**, 041402; R. Temirov, S. Soubatch, A. Luican and F. S. Tautz, *Nature*, 2006, **444**, 350; A. Hauschild, K. Karki, B. C. C. Cowie, M. Rohlfing, F. S. Tautz and M. Sokolowski, *Phys. Rev. Lett.*, 2005, **94**, 036106; M. Eremtchenko, J. A. Schaefer and F. S. Tautz, *Nature*, 2003, **425**, 602.
9 M. A. Loi, E. Da Como, F. Dinelli, M. Murgia, R. Zamboni, F. Biscarini and M. Muccini, *Nat. Mater.*, 2005, **4**, 81.
10 S. Kowarik, A. Gerlach, S. Sellner, F. Schreiber, L. Cavalcanti and O. Konovalov, *Phys. Rev. Lett.*, 2006, **96**, 125504.
11 S. E. Fritz, S. M. Martin, C. D. Frisbie, M. D. Ward and M. F. Toney, *J. Am. Chem. Soc.*, 2004, **126**, 4084; H. C. Yang, T. J. Shin, M.-M. Ling, K. Cho, C. Y. Ryu and Z. N. Bao, *J. Am. Chem. Soc.*, 2005, **127**, 11542; H. Yoshida and N. Sato, *Appl. Phys. Lett.*, 2006, **89**, 101919; H. Yoshida, K. Inaba and N. Sato, *Appl. Phys. Lett.*, 2007, **90**, 181930; T. Kakudate, N. Yoshimoto and N. Sato, *Appl. Phys. Lett.*, 2007, **90**, 081903.
12 G. R. Dholakia, M. Meyyappan, A. Facchetti and T. J. Marks, *Nano Lett.*, 2006, **6**, 2447.
13 W. Chen, L. Wang, D. C. Qi, S. Chen, X. Y. Gao and A. T. S. Wee, *Appl. Phys. Lett.*, 2006, **88**, 184102; W. Chen, C. Huang, X. Y. Gao, L. Wang, D. C. Qi, S. Chen, H. L. Zhang, K. P. Zhang, Z. K. Chen and A. T. S. Wee, *J. Phys. Chem. B*, 2006, **110**, 26075; W. Chen, X. Y. Gao, D. C. Qi, S. Chen, Z. K. Chen and A. T. S. Wee, *Adv. Funct. Mater.*, 2007, **17**, 1339; W. Chen, H. Huang, S. Chen, L. Chen, H. L. Zhang, X. Y. Gao and A. T. S. Wee, *Appl. Phys. Lett.*, 2007, **91**, 114102; W. Chen, S. Chen, H. Huang, D. C. Qi, X. Y. Gao and A. T. S. Wee, *Appl. Phys. Lett.*, 2008, **92**, 063308.
14 G. E. Thayer, J. T. Sadowski, F. M. zu Heringdorf, T. Sakurai and R. M. Tromp, *Phys. Rev. Lett.*, 2005, **95**, 256106.
15 S. Tsuzuki, K. Honda, T. Uchimaru, M. Mikami and K. Tanabe, *J. Am. Chem. Soc.*, 2002, **124**, 104; S. Tsuzuki, K. Honda and R. Azumi, *J. Am. Chem. Soc.*, 2002, **124**, 12200; S. Tsuzuki, K. Honda, T. Uchimaru, M. Mikami and K. Tanabe, *J. Am. Chem. Soc.*, 2000, **122**, 3746; S. Tsuzuki, K. Honda, T. Uchimaru, M. Mikami and K. Tanabe, *J. Am. Chem. Soc.*, 2000, **122**, 11450.
16 R. Ruiz, B. Nicket, N. Koch, L. C. Feldman, R. F. Haglund, A. Kahn and G. Scoles, *Phys. Rev. B*, 2003, **67**, 125406.
17 G. Koller, S. Berkebile, M. Oehzelt, P. Puschnig, C. Ambrosch-Draxl, F. P. Netzer and M. G. Ramsey, *Science*, 2007, **317**, 351.
18 S. R. Forrest, *Chem. Rev.*, 1997, **97**, 1793.
19 H. L. Zhang, W. Chen, L. Chen, H. Huang, X. S. Wang, J. Yuhara and A. T. S. Wee, *Small*, 2007, **3**, 2015.
20 J. Repp, G. Meyer, S. M. Stojković, A. Gourdon and C. Joachim, *Phys. Rev. Lett.*, 2005, **94**, 026803.
21 H. L. Zhang, W. Chen, H. Huang, L. Chen and A. T. S. Wee, *J. Am. Chem. Soc.*, 2008, **130**, 2720.
22 F. Ortmann, W. G. Schmidt and F. Bechstedt, *Phys. Rev. Lett.*, 2005, **95**, 186101; P. Sony, P. Puschnig, D. Nabok and C. Ambrosch-Draxl, *Phys. Rev. Lett.*, 2007, **99**, 176401.
23 N. Koch, A. Vollmer, I. Salzmann, B. Nickel, H. Weiss and J. P. Rabe, *Phys. Rev. Lett.*, 2006, **96**, 156803.
24 C. B. France, F. AndrewFrame and B. A. Parkinson, *Langmuir*, 2006, **22**, 7507; C. B. France and B. A. Parkinson, *Appl. Phys. Lett.*, 2003, **82**, 1194.
25 S. W. Hla, K. F. Braun, B. Wassermann and K. H. Rieder, *Phys. Rev. Lett.*, 2004, **93**, 208302.

This journal is © The Royal Society of Chemistry 2008